Triplet Relationship Guided Sampling Consensus for Robust Model Estimation

Hanlin Guo, Yang Lu, *Member, IEEE*, Guobao Xiao, *Member, IEEE*, Shuyuan Lin, and Hanzi Wang, *Senior Member, IEEE*

***Abstract*—RANSAC (RANdom SAmple Consensus) is a widely used robust estimator for estimating a geometric model from feature matches in an image pair. Unfortunately, it becomes less effective when initial input feature matches (i.e., input data) are corrupted by a large number of outliers. In this paper, we propose a new robust estimator (called TRESAC) for model estimation, where data subsets are sampled with the guidance of the triplet relationships, which involve high relevance and local geometric consistency. Each triplet consists of three data, whose relationships satisfy spatial consistency constraints. Therefore, the triplet relationships can be used to effectively initialize and refine the sampling process. With the advantage of the triplet relationships, TRESAC significantly alleviates the influence of outliers and also improves the computational efficiency of model estimation. Experimental results on four challenging datasets show that TRESAC can achieve superior performance on both estimation accuracy and computational efficiency against several other state-of-the-art methods.**

***Index Terms*—Outlier removal, robust estimator, sampling.**

I. Introduction

MODEL estimation is an important step in various computer vision and robotics tasks, including image registration [1]–[4], 3-D reconstruction [5], [6], motion estimation [7], [8], and simultaneous location and mapping [9], [10]. One of the main challenges during model estimation is that most input data are inevitably corrupted by outliers due to the limitations of data acquisition systems and preprocessing techniques. The estimated model parameters from these corrupted data may be severely biased, which could lead to a negative impact on final results in many practical applications.

Manuscript received December 27, 2021; revised February 8, 2022; accepted February 10, 2022. Date of publication February 25, 2022; date of current version March 30, 2022. This work was supported in part by the National Natural Science Foundation of China under Grants U21A20514, 61872307, 62002302, and 62072223, and in part by the Natural Science Fund of Fujian Province under Grant 2020J01005. The associate editor coordinating the review of this manuscript and approving it for publication was Dr. Ferdous Sohel. *(Corresponding author: Hanzi Wang.)*

This work involved human subjects or animals in its research. The author(s) confirm(s) that all human/animal subject research procedures and protocols are exempt from review board approval.

Hanlin Guo, Yang Lu, and Hanzi Wang are with the Fujian Key Laboratory of Sensing and Computing for Smart City, School of Informatics, Xiamen University, Xiamen 361005, China (e-mail: hanlinguo@stu.xmu.edu.cn; luyang@xmu.edu.cn; hanzi.wang@ieee.org).

Shuyuan Lin is with the College of Information Science and Technology/College of Cyber Security, Jinan University, Guangzhou 510632, China (e-mail: swin.shuyuan.lin@gmail.com).

Guobao Xiao is with the College of Computer and Control Engineering, Minjiang University, Fuzhou 350108, China (e-mail: gbx@mju.edu.cn).

Digital Object Identifier 10.1109/LSP.2022.3154675

Many robust estimators have been proposed for model estimation, and they can be coarsely divided into two categories, i.e., nonparametric-based algorithms and parametric-based algorithms. Nonparametric-based algorithms (such as, RPM [11], LPM [12] and GFEMR [13]) usually exploit specified functions based on various geometric priors (e.g., spatial consistency information [14]) to distinguish inliers from outliers. They use the obtained inliers for model estimation. Parametric-based algorithms (such as, RANSAC [15], Adaptive-RANSAC [16], RSW-LTS [17] and Hierarchical-RANSAC [18]) typically operate in a hypothesize-and-verify scheme, which iteratively performs the model hypothesis generation and model verification steps until they obtain a good solution. They estimate models from input data and remove outliers simultaneously. While these robust estimators are effective for general cases of model estimation, their performance dramatically degenerates for data with high outlier ratios. Specifically, for parametric-based algorithms such as RANSAC, the computational efficiency tend to be affected heavily by outlier ratios. For nonparametric-based algorithms, high outlier ratios may also result in the problem that the spatial consistency of inliers is hard to be captured, leading to seriously degraded performance of model estimation.

The traditional pairwise relationship is commonly used for robust estimation by combining the spatial consistency constraint, which assumes that only inliers are likely to be consistent with each other [19]. However, outliers may be misjudged as inliers by using the pairwise relationship since outliers may have similar local geometric relationships (see Fig. 1(a)). To improve the robustness, we extend the pairwise relationship to the triplet relationship, and all pairwise relationships within a triplet (including three data) satisfy the spatial consistency constraint. Thus, the triplet relationships can help detect potential outliers (see Fig. 1(b)) for robust estimation.

In this paper, we propose an efficient and robust estimator called Triplet RElationship guided SAmpling Consensus (TRESAC) for model estimation between image pairs. The key idea of TRESAC is that it utilizes the triplet relationships to guide the sampling process of effective data subsets for robust estimation. Specifically, we firstly analyze the triplet relationships among input feature matches (i.e., input data), and obtain a series of triplet sets of feature matches. Each triplet consists of three data, whose relationships satisfy the spatial consistency constraints. Then, we propose an initial data subset selection strategy (i.e., IDSS), which computes the sampling weights of input data based on the triplets and uses them to effectively sample an initial data

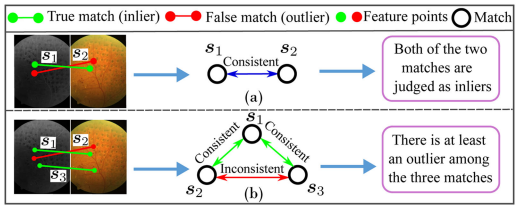

Fig. 1. Comparisons of (a) the pairwise relationship and (b) the triplet relationship for the task of robust model estimation. In (a), $\boldsymbol{s}_1$ and $\boldsymbol{s}_2$ satisfy the spatial consistency constraint, because the corresponding feature points of $\boldsymbol{s}_1$ and $\boldsymbol{s}_2$ are both spatially close to each other. Thus, both of them are judged as inliers. In (b), $\boldsymbol{s}_1$ and $\boldsymbol{s}_2$, $\boldsymbol{s}_1$ and $\boldsymbol{s}_3$ satisfy the spatial consistency constraint, while $\boldsymbol{s}_2$ and $\boldsymbol{s}_3$ do not. Therefore, due to the multiple constraints in the triplet, the outliers can be effectively detected among the three matches.

subset. After that, we propose a data subset refinement strategy (i.e., DSR), which adopts a previous iterative scheme [20] and a new stop criterion derived from the triplet relationships, to further improve the sampling performance. At last, we generate a significant model according to the finally obtained data subset, and use the model to find the inliers and outliers. We summarize the main contributions of this paper as follows:

- We investigate the triplet relationships, which explore the spatial consistency among feature matches to reflect their local correlation in images for robust estimation.
- Based on the triplet relationships, we propose a novel robust estimator, which can not only efficiently sample promising initial data subsets to generate significant model hypotheses, but also boost the effectiveness of the model hypotheses to improve the robustness to outliers.

Experimental results on challenging datasets show the superiority of the proposed method over other competing methods.

II. The Proposed Method

A. Triplet relationships for Robust Estimation

Unlike the previous methods that use consistency constraints in the pairwise relationships [14], [19], we propose to find the triplet relationships of feature matches by using spatial consistency constraints and incorporate it into robust estimation.

Given a feature match $\boldsymbol{s}_i = (\boldsymbol{x}_i, \boldsymbol{y}_i)$ from input data $\mathcal{S} = \{\boldsymbol{s}_i = (\boldsymbol{x}_i, \boldsymbol{y}_i)\}_{i=1}^{N}$ of N feature matches in a pair of images, we search for the K-nearest neighbors $\mathcal{N}_{\boldsymbol{x}_i}$ and $\mathcal{N}_{\boldsymbol{y}_i}$ of the feature points $\boldsymbol{x}_i$ and $\boldsymbol{y}_i$ based on their spatial relationships, respectively. For a feature point $\boldsymbol{x}_i$, we define its triplet relationship among the feature points from $\mathcal{S}$ as follows.

Definition 1 (Triplet Relationship): A triplet $\Delta_{\boldsymbol{x}_i\boldsymbol{x}_j\boldsymbol{x}_k}$ includes three feature points, i.e., $\Delta_{\boldsymbol{x}_i\boldsymbol{x}_j\boldsymbol{x}_k} = (\boldsymbol{x}_i, \boldsymbol{x}_j, \boldsymbol{x}_k)$, if and only if the relationships of $\boldsymbol{x}_i$, $\boldsymbol{x}_j$, and $\boldsymbol{x}_k$ satisfy:

$$\mathbf{1}_{\boldsymbol{x}_i \in \mathcal{N}_{\boldsymbol{x}_j}} \times \mathbf{1}_{\boldsymbol{x}_k \in \mathcal{N}_{\boldsymbol{x}_i}} \times \mathbf{1}_{\boldsymbol{x}_j \in \mathcal{N}_{\boldsymbol{x}_k}} = 1, \tag{1}$$

where $\mathbf{1}_{\boldsymbol{x} \in \mathcal{N}}$ represents an indicator function whose value is equal to 1 if $\boldsymbol{x} \in \mathcal{N}$ and 0 otherwise.

It is possible that there are more than three feature points that satisfy (1) for the feature point $\boldsymbol{x}_i$ (i.e., more than one triplet associated with $\boldsymbol{x}_i$). Thus, we denote the triplet set of $\boldsymbol{x}_i$ as $\Omega_{\boldsymbol{x}_i} = \{(\Delta_{\boldsymbol{x}_i\boldsymbol{x}_j\boldsymbol{x}_k})\}$. The other feature point $\boldsymbol{y}_i$ of $\boldsymbol{s}_i$ has the similar definition as $\boldsymbol{x}_i$. Its triplet set is denoted as $\Omega_{\boldsymbol{y}_i} = \{(\Delta_{\boldsymbol{y}_i\boldsymbol{y}_j\boldsymbol{y}_k})\}$. If the feature points $\boldsymbol{x}_i$ and $\boldsymbol{y}_i$ of a feature match $\boldsymbol{s}_i$ have the corresponding triplets $\Delta_{\boldsymbol{x}_i\boldsymbol{x}_j\boldsymbol{x}_k}$ and $\Delta_{\boldsymbol{y}_i\boldsymbol{y}_j\boldsymbol{y}_k}$, the three feature matches $\boldsymbol{s}_i$, $\boldsymbol{s}_j$ and $\boldsymbol{s}_k$ are regarded as a triplet of feature matches $\Delta_{\boldsymbol{s}_i\boldsymbol{s}_j\boldsymbol{s}_k} = (\boldsymbol{s}_i, \boldsymbol{s}_j, \boldsymbol{s}_k)$ that associates with $\boldsymbol{s}_i$ (an example is shown in Fig. 2). Note that a feature match $\boldsymbol{s}_i$ may also associate with multiple triplets. Thus, we denote the triplet set of $\boldsymbol{s}_i$ as $\Omega_{\boldsymbol{s}_i} = \{(\Delta_{\boldsymbol{s}_i\boldsymbol{s}_j\boldsymbol{s}_k})\}$. Based on the above analysis, we generate the triplet sets for each of input data $\mathcal{S}$, and denote them as $\mathcal{A} = \{(\Omega_{\boldsymbol{s}_i})\}$. Note that, the authors in [21] use the triplet relationships for clustering data, while we use it for sampling data subsets. In addition, the authors in [22] used the matched triangle pairs, where each triangle consists of three feature points, to find potential true matches. In contrast, we use the triplets of feature matches to compute the weight set of feature matches, during the data subset sampling process.

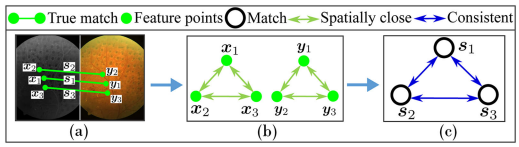

Fig. 2. Illustration of identifying triplets for feature matches. (a) Three feature matches $(\boldsymbol{s}_1, \boldsymbol{s}_2, \boldsymbol{s}_3)$ and $\boldsymbol{s}_i = (\boldsymbol{x}_i, \boldsymbol{y}_i)$. (b) Two triplets of the feature points $\Delta_{\boldsymbol{x}_1\boldsymbol{x}_2\boldsymbol{x}_3}$ and $\Delta_{\boldsymbol{y}_1\boldsymbol{y}_2\boldsymbol{y}_3}$. (c) The triplet of feature matches $\Delta_{\boldsymbol{s}_1\boldsymbol{s}_2\boldsymbol{s}_3}$.

B. Initial Data Subset Selection Strategy

The triplet relationships incorporate the complementarity of multiple constraints within triplets, and they can significantly alleviate the sensitivity to outliers. Thus, we present an initial data subset selection strategy by taking advantage of the triplet relationships to effectively capture the sampling weight set of data, to sample a promising initial data subset.

Given two feature matches $\boldsymbol{s}_i$ and $\boldsymbol{s}_j$, we can calculate their compatibility score by pairwise relationships as follows [23]:

$$f(\boldsymbol{s}_i, \boldsymbol{s}_j) = \exp\left(-(||\boldsymbol{y}_j - \boldsymbol{y}_i||_2 - ||\boldsymbol{x}_j - \boldsymbol{x}_i||_2)^2\right). \tag{2}$$

By investigating (2), a pair of feature matches, i.e., $\boldsymbol{s}_i = (\boldsymbol{x}_i, \boldsymbol{y}_i)$ and $\boldsymbol{s}_j = (\boldsymbol{x}_j, \boldsymbol{y}_j)$, satisfying the spatial consistency constraint, will get a high compatibility score, and thus they are considered to have a high probability of being inliers. However, computing the compatibility scores based on the pairwise relationships may not be robust to outliers, especially for a large number of outliers. To alleviate the influence of outliers, we incorporate the triplet relationships into the compatibility score calculation of feature matches. Given a triplet $\Delta_{\boldsymbol{s}_i\boldsymbol{s}_j\boldsymbol{s}_k}$, based on (2), the compatibility score of feature matches within the triplet is defined as follows:

$$c(\boldsymbol{s}_i, \boldsymbol{s}_j, \boldsymbol{s}_k) = f(\boldsymbol{s}_i, \boldsymbol{s}_j) + f(\boldsymbol{s}_j, \boldsymbol{s}_k) + f(\boldsymbol{s}_k, \boldsymbol{s}_i). \tag{3}$$

According to (3), if all three feature matches within the triplet are inliers, the compatibility score is high; Otherwise, the compatibility score is low.

Based on the compatibility scores derived from the triplet set $\mathcal{A}$, we then compute the sampling weight $w(\boldsymbol{s}_i)$ of a datum $\boldsymbol{s}_i$ from a set of N data $\mathcal{S} = \{\boldsymbol{s}_i = (\boldsymbol{x}_i, \boldsymbol{y}_i)\}_{i=1}^{N}$ as follows:

$$w(\boldsymbol{s}_i) = \begin{cases} \max\{c(\boldsymbol{s}_i, \boldsymbol{s}_j, \boldsymbol{s}_k)\}, & \text{if } \Delta_{\boldsymbol{s}_i\boldsymbol{s}_j\boldsymbol{s}_k} \in \mathcal{A}, \\ 0, & \text{otherwise}, \end{cases} \tag{4}$$

where $\max\{c(\boldsymbol{s}_i, \boldsymbol{s}_j, \boldsymbol{s}_k)\}$ denotes the maximum value of the compatibility scores of the triplets that associate with a datum

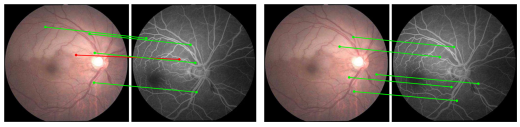

Fig. 3. The sampled data subsets respectively obtained by the initial data subset selection strategy (left) and the data subset refinement strategy (right). Inliers and outliers are denoted in the red and green colors, respectively.

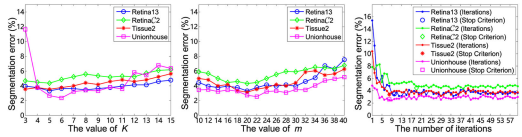

Fig. 4. Comparison results obtained by the proposed TRESAC with different settings of the parameters on the four representative image pairs.

$\boldsymbol{s}_i$. In contrast, if a datum $\boldsymbol{s}_i$ is not associated with any triplet, $w(\boldsymbol{s}_i)$ is set to be zero. Therefore, we select an initial data subset according to the sampling weights, i.e., $\boldsymbol{s}_i$ is more likely to be selected compared with $\boldsymbol{s}_j$, if $w(\boldsymbol{s}_i) > w(\boldsymbol{s}_j)$, to generate a significant model hypothesis for robust estimation.

C. Data Subset Refinement Strategy

By the initial data subset selection strategy, we can prevent a majority of outliers from being selected during sampling. However, outliers may also be selected into a data subset, especially when the input feature matches only contain a few inliers, yielding ineffective data subsets for model estimation (see the left of Fig. 3 for an example).

To find enough inliers to form effective data subsets, we introduce a data subset refinement strategy by adopting an iterative scheme. Specifically, given a model hypothesis θ_ℓ (generated by a sampled data subset), we first compute the residual values $\{r(\boldsymbol{s}_i, \theta_\ell)\}_{i=1}^N$ between the model hypothesis θ_ℓ and the input data $\mathcal{S} = \{\boldsymbol{s}_i\}_{i=1}^N$ based on the Sampson distance [24]. Then, we sort the residual values in an ascending order. After that, according to the sorted residual values, we sort all the input data and sample a data subset around the m-th datum from the sorted data to generate a new model hypothesis. We iteratively perform these steps until we obtain a stable solution. Similar to [20], we determine whether the data subset refinement process converges based on the last three iterations, and we also use a parameter (i.e., $MaxIter$) for the maximum number of iterations. However, the difference is that we use the weight values derived from the triplet relationships of sampled data as a condition for the stop criterion, to reduce the sensitivity to outliers. In contrast, the authors in [20] directly utilize the residual values of sampled data in the stop criterion. Specifically, we formulate the stop criterion I_{stop} as:

$$I_{stop} = \left(\frac{1}{h}\sum_{j=m-h+1}^{m} w(\boldsymbol{s}_j^{\theta_{(\ell-1)}}) < w(\boldsymbol{s}_m^{\theta_\ell})\right) \wedge \left(\frac{1}{h}\sum_{j=m-h+1}^{m} w(\boldsymbol{s}_j^{\theta_{(\ell-2)}}) < w(\boldsymbol{s}_m^{\theta_\ell})\right), \tag{5}$$

where $\boldsymbol{s}_m^{\theta_\ell}$ is the m-th datum from the sorted data derived from the sorted residuals in the ℓ-th iteration; $w(\cdot)$ is the weight of a datum computed by (4). The criterion indicates that the data subsets sampled from the last three iterations are more likely to belong to the same model and then the iteration is stopped. Thus, we can further improve the performance of data subset sampling and obtain an effective data subset to generate a significant model hypothesis as the estimated model (see the right of Fig. 3 for an example). Finally, we can distinguish inliers from outliers according to the estimated model.

III. Experiments

A. Datasets and evaluation Metric

Datasets: We conduct the experiments on four datasets, i.e., the RETINA [11], [25], MMRI [26], TISSUE [27] and AdelaideRMF datasets [28]. From the RETINA, MMRI and TISSUE datasets, we respectively selected 15 representative image pairs for the affine model estimation. We also evaluate on the challenging AdelaideRMF dataset that contains 19 image pairs for the fundamental matrix estimation.

Evaluation Metric: The segmentation error (SE) is computed as [20], [29]: $SE = \frac{the\ number\ of\ mislabeled\ data}{the\ total\ number\ of\ input\ data} \times 100\%$. The performance of the robust estimation is better when the value of SE is lower. All experiments were repeated 50 times and were run on MS Windows 10 with Intel Core i7-7700 CPU @$3.6GHz$ and $16GB$ RAM.

B. Analysis for the Proposed TRESAC

1) Parameter Analysis: There are five parameters in TRESAC: K, m, p, h, and $MaxIter$. K is used for the generation of K-nearest neighbors of each feature point. m is the minimal tolerable number of inliers in a model. p is the size of the minimal subset, and it is the minimal number of the data required to generate a model hypothesis (e.g., $p = 3$ for an affine model and $p = 8$ for an fundamental matrix [24]). h is the size of a data subset. We selected $h = p + 2$ data to generate a model hypothesis as in [20], due to its effectiveness. We test different parameter values for K, m and $MaxIter$ on the four selected image pairs (i.e., Retina13, Retina$\mathcal{C}$2, Tissue2, and Unionhouse) from the four aforementioned datasets, respectively. We report the segmentation errors in Fig. 4.

As can be seen, for K and m, TRESAC is able to obtain low segmentation errors on the four image pairs when $K = 5$ and $m = 20$, respectively. For $MaxIter$, TRESAC is able to obtain relatively stable results when $33 \leq MaxIter \leq 60$. Thus, we set $K = 5$, $m = 20$, and $MaxIter = 50$ for TRESAC in all the experiments. Note that for the analysis of parameter $MaxIter$, we use different numbers of the iterations in TRESAC to stop the iteration process. Thus, we also use the proposed stop criterion in TRESAC to stop the iteration process. We show the segmentation errors in the right of Fig. 4. As can be seen, TRESAC with the proposed stop criterion achieves low segmentation errors, when the numbers of the iterations are 10, 19, 8, and 8 on the Retina13, Retina$\mathcal{C}$2, Tissue2, and Unionhouse image pairs, respectively. This shows the effectiveness of the proposed stop criterion.

2) Ablation Study: To show the contributions of the initial data subset selection strategy (IDSS) and the data subset refinement strategy (DSR) to TRESAC, we test three different versions of TRESAC, including TRESAC with both IDSS and DSR

TABLE I
SEGMENTATION ERRORS (IN PERCENTAGE) AND RUNNING TIME (IN SECONDS) FOR TRESAC AND ITS VARIANTS ON THE RETINA DATASET

	TRGSAC	TRGSAC+IDSS	TRGSAC+DSR	TRGSAC+PR	TRGSAC+RBSC
Avg.	**3.505**	6.731	6.479	5.238	5.039
Std.	**1.164**	4.313	2.385	2.087	2.084
Time	**0.049**	0.016	0.042	0.056	0.054

TABLE II
SEGMENTATION ERRORS (IN PERCENTAGE) AND RUNNING TIME (IN SECONDS) OBTAINED BY THE SEVEN METHODS FOR OUTLIER REMOVAL. '#' DENOTES THE AVERAGE OUTLIER RATIOS OF ALL DATA IN A DATASET

Datasets ('#')		RPM	LPM	GFEMR	RANSAC	RANSAC++	EES	TRGSAC
RETINA (53.485%)	Avg.	6.447	11.018	3.768	8.055	5.509	3.861	**3.505**
	Std.	5.984	7.151	1.992	**0.484**	1.149	3.218	1.164
	Time	2.976	**0.002**	0.808	0.869	0.214	0.014	0.049
MMRI (65.643%)	Avg.	7.432	15.009	5.724	7.657	6.651	6.273	**5.063**
	Std.	8.128	9.716	3.844	2.935	**2.312**	3.751	3.063
	Time	3.150	**0.004**	1.201	7.954	0.198	0.018	0.070
AdelaideRMF (44.906%)	Avg.	7.879	7.190	4.958	6.816	5.984	4.634	**3.542**
	Std.	3.912	2.627	3.050	**2.006**	2.315	3.758	2.251
	Time	6.068	**0.003**	2.567	6.817	0.362	0.031	0.075
TISSUE (32.137%)	Avg.	7.511	8.361	4.915	8.939	6.821	5.550	**4.584**
	Std.	3.071	5.065	2.998	4.023	**2.354**	2.105	2.357
	Time	2.385	**0.001**	0.725	0.631	0.297	0.011	0.036

(i.e., TRESAC is used as a benchmark), TRESAC+IDSS with only IDSS (i.e., TRESAC without using DSR), TRESAC+DSR with only DSR (i.e., TRESAC using the random sampling strategy instead of using DSR). To compare the triplet relationships, we test a version (i.e., TRESAC+PR) with the pairwise relationships (PR). In addition, we test a version (TRESAC+RBSC) with the residual-based stop criterion (RBSC) [20] to compare with the proposed stop criterion.

We show the quantitative results obtained by different versions of TRESAC in Table I. We use the challenging RETINA dataset for evaluation. As we can see, TRESAC+IDSS use less running time than TRESAC+DSR for robust estimation. And TRESAC+IDSS without using DSR has an increase in the average segmentation error by 3.226%, while TRESAC+DSR without using IDSS has an increase in the average segmentation error by 2.974%. Thus, DSR contributes more than IDSS to improve the robust estimation performance of TRESAC. For TRESAC and TRESAC+PR, TRESAC can achieve better performance than TRESAC+PR considering both segmentation errors and running time. This shows the effectiveness of the triplet relationships for robust estimation. For different stop criteria, TRESAC is able to achieve superior segmentation accuracy over TRESAC+RBSC, while they spend similar running time. Thus, this shows that the proposed stop criterion is more effective than RBSC for robust estimation.

C. Quantitative Results

We evaluate the performance of the proposed TRESAC on the RETINA, MMRI, TISSUE and AdelaideRMF datasets, and we compare TRESAC with the classic RANSAC [15] and five state-of-the-art robust estimation methods, including RPM [11], LPM [12], GFEMR [13], RANSAC++ [29], and EES [30] The quantitative comparisons of all the seven methods on the four datasets are shown in Table II. As we can see, TRESAC achieves the lowest average segmentation errors on each of the four datasets among all the methods. Specifically, among the nonparameters-based methods (i.e., RPM, LPM and GFEMR), GFEMR achieves better segmentation results for outlier removal but it achieves higher average segmentation errors than those

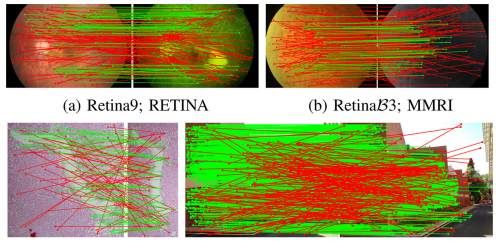

(a) Retina9; RETINA (b) Retina33; MMRI

(c) Tissue12; TISSUE (d) Unihouse; AdelaideRMF

Fig. 5. Qualitative results obtained by TRESAC on the four selected image pairs from four datasets, respectively. The outlier ratios (and the number of feature matches) for the four image pairs in (a), (b), (c), and (d) are 71.515% (165), 85.532% (235), 51.908% (131), and 16.555%(2084), respectively. The inliers and outliers are respectively shown with the green and red colors.

obtained by TRESAC on the four datasets. For the parameters-based methods (i.e., RANSAC, RANSAC++, TRESAC, and EES), the segmentation results obtained by TRESAC are more accurate than those obtained by the other three methods. This is because that TRESAC samples initial data subsets from potential inliers by using IDSS and it also benefits from the effectiveness of DSR for the data subset refinement, to generate a significant model for robust estimation. TRESAC achieves stable results on the four datasets with low standard deviations of segmentation errors. For the computational time, TRESAC achieves the third-lowest running time on each of the four datasets among the seven methods, and it is much more efficient than the classic RANSAC. This is because that the computational complexity of TRESAC is mainly governed by the step of searching the K-nearest neighbors of feature points and it is about $O((K+N)\log N)$, where N is the number of feature matches. However, RANSAC is mainly affected by high outlier ratios.

D. Qualitative Results

We show the segmentation results obtained by TRESAC on the four challenging image pairs in Fig. 5. The mean segmentation errors (and running time) obtained by TRESAC are 5.053% (0.075 s), 4.543% (0.084 s), 4.582% (0.054 s), and 6.737% (0.553 s), respectively. From these results and Fig. 5, we can see that the inliers are segmented effectively from the outliers on each image pair, and the used running time is relatively low, mainly due to the effectiveness of the triple relationship guided sampling for robust estimation.

IV. CONCLUSION

We propose a novel robust estimator TRESAC for model estimation even in the presence of a large number of outliers. We first investigate the triplet relationships by combining the multiple spatial consistency constraints to detect potential inliers for robust estimation. Due to the complementarity of multiple constraints, the triplet relationships are more beneficial than the pairwise relationships, when computing sampling weight set of input data, for generating effective data subsets. The proposed data subset initialization strategy and the data subset refinement strategy are verified to be effective mainly due to the advantage of the triplet relationships. Experimental results on four challenging datasets show that TRESAC outperforms several other state-of-the-art robust estimation methods.

REFERENCES

[1] I. Aganj and B. Fischl, "Multimodal image registration through simultaneous segmentation," *IEEE Signal. Process. Lett.*, vol. 24, no. 11, pp. 1661–1665, Nov. 2017.

[2] N. Martinel, C. Micheloni, and G. L. Foresti, "Robust painting recognition and registration for mobile augmented reality," *IEEE Signal. Process. Lett.*, vol. 20, no. 11, pp. 1022–1025, Nov. 2013.

[3] Z. Ghassabi, J. Shanbehzadeh, and A. Mohammadzadeh, "A structure-based region detector for high-resolution retinal fundus image registration," *Biomed. Signal Process. Control*, vol. 23, pp. 52–61, 2016.

[4] S. Du, N. Zheng, G. Meng, and Z. Yuan, "Affine registration of point sets using ICP and ICA," *IEEE Signal. Process. Lett.*, vol. 15, pp. 689–692, 2008.

[5] J. Ma, Y. Ma, J. Zhao, and J. Tian, "Image feature matching via progressive vector field consensus," *IEEE Signal. Process. Lett.*, vol. 22, no. 6, pp. 767–771, Jun. 2015.

[6] J. Yang, Z. Huang, S. Quan, Z. Qi, and Y. Zhang, "SAC-COT: Sample consensus by sampling compatibility triangles in graphs for 3-D point cloud registration," *IEEE Trans. Geosci. Remote Sens*., vol. 60, 2022, Art no. 5700115.

[7] Y. C. Chung and Z. He, "Reliability analysis for global motion estimation," *IEEE Signal. Process. Lett.*, vol. 16, no. 11, pp. 977–980, Nov. 2009.

[8] Y. Zhang, B. Luo, and L. Zhang, "Permutation preference based alternate sampling and clustering for motion segmentation," *IEEE Signal. Process. Lett.*, vol. 25, no. 3, pp. 432–436, Mar. 2018.

[9] H. Deusch, S. Reuter, and K. Dietmayer, "The labeled multi-Bernoulli SLAM filter," *IEEE Signal. Process. Lett.*, vol. 22, no. 10, pp. 1561–1565, Oct. 2015.

[10] R. Li, J. Sun, D. Gong, Y. Zhu, H. Li, and Y. Zhang, "ARSAC: Efficient model estimation via adaptively ranked sample consensus," *Neurocomputing*, vol. 328, pp. 88–96, 2019.

[11] G. Wang, Z. Wang, Y. Chen, and W. Zhao, "Robust point matching method for multimodal retinal image registration," *Biomed. Signal Process. Control*, vol. 19, pp. 68–76, 2015.

[12] J. Ma, J. Zhao, J. Jiang, H. Zhou, and X. Guo, "Locality preserving matching," *Int. J. Comput. Vision.*, vol. 127, no. 5, pp. 512–531, 2019.

[13] J. Wang *et al.*, "Gaussian field estimator with manifold regularization for retinal image registration," *Signal Process.*, vol. 157, pp. 225–235, 2019.

[14] S. Quan and J. Yang, "Compatibility-guided sampling consensus for 3-D point cloud registration," *IEEE Trans. Geosci. Remote Sens.*, vol. 58, no. 10, pp. 7380–7392, Oct. 2020.

[15] M. A. Fischler and R. C. Bolles, "Random sample consensus: A paradigm for model fitting with applications to image analysis and automated cartography," *Commun. ACM*, vol. 24, no. 6, pp. 381–395, 1981.

[16] Z. Hossein-Nejad and M. Nasri, "A-RANSAC: Adaptive random sample consensus method in multimodal retinal image registration," *Biomed. Signal Process. Control*, vol. 45, pp. 325–338, 2018.

[17] E. P. Ong *et al.*, "A robust outlier elimination approach for multimodal retina image registration," in *Proc. Int. Conf. Med. Image Comput. Comput.-Assist. Interv.*, pp. 329–337, 2015.

[18] X. Gao, J. Luo, K. Li, and Z. Xie, "Hierarchical RANSAC-based rotation averaging," *IEEE Signal. Process. Lett.*, vol. 27, pp. 1874–1878, 2020.

[19] H. M. Sahloul, S. Shirafuji, and J. Ota, "An accurate and efficient voting scheme for a maximally all-inlier 3D correspondence set," *IEEE Trans. Pattern Anal. Mach. Intell.*, vol. 43, no. 7, pp. 2287–2298, Jul. 2021.

[20] R. B. Tennakoon, A. Bab-Hadiashar, Z. Cao, R. Hoseinnezhad, and D. Suter, "Robust model fitting using higher than minimal subset sampling," *IEEE Trans. Pattern Anal. Mach. Intell.*, vol. 38, no. 2, pp. 350–362, Feb. 2016.

[21] J. Liang, J. Yang, M.-M. Cheng, P. L. Rosin, and L. Wang, "Simultaneous subspace clustering and cluster number estimating based on triplet relationship," *IEEE Trans. Image Process.*, vol. 28, no. 8, pp. 3973–3985, Aug. 2019.

[22] H. Liu, H. Zhang, Z. Wang, and Y. Zheng, "Feature matching based on triangle guidance and constraints," *Int. J. Pattern Recognit. Artif. Intell.*, vol. 32, no. 8, 2018, Art. no. 1855014.

[23] J. Li, Q. Hu, and M. Ai, "GESAC: Robust graph enhanced sample consensus for point cloud registration," *ISPRS J. Photogramm. Remote Sens.*, vol. 167, pp. 363–374, 2020.

[24] R. Hartley and A. Zisserman, *Multiple View Geometry in Computer Vision*. Cambridge, U.K.: Cambridge Univ. Press, 2004.

[25] J. Ma, J. Jiang, C. Liu, and Y. Li, "Feature guided Gaussian mixture model with semi-supervised em and local geometric constraint for retinal image registration," *Inf. Sci.*, vol. 417, pp. 128–142, 2017.

[26] H. Guo *et al.*, "Motion consistency guided robust geometric model fitting with severe outliers," *IEEE Trans. Ind. Electron.*, vol. 69, no. 4, pp. 4065–4075, Apr. 2022.

[27] C. W. Wang and H. C. Chen, "Improved image alignment method in application to X-ray images and biological images," *Bioinformatics*, vol. 29, no. 15, pp. 1879–1887, 2013.

[28] H. S. Wong, T. J. Chin, J. Yu, and D. Suter, "Dynamic and hierarchical multi-structure geometric model fitting," in *Proc. Int. Conf. Comput. Vis.*, 2011, pp. 1044–1051.

[29] Q. H. Tran, T. J. Chin, G. Carneiro, M. S. Brown, and D. Suter, "In defence of RANSAC for outlier rejection in deformable registration," in *Proc. Eur. Conf. Comput. Vis.*, 2012, pp. 274–287.

[30] A. Fan, J. Ma, X. Jiang, and H. Ling, "Efficient deterministic search with robust loss functions for geometric model fitting," *IEEE Trans. Pattern Anal. Mach. Intell*., early access, Sep. 21, 2021, doi: 10.1109/TPAMI.2021.3109784.